

DIRECTIVITY PATTERNS CONTROLLING THE AUDITORY SOURCE DISTANCE

Florian Wendt, Matthias Frank, Franz Zotter, Robert Höldrich

Institute of Electronic Music and Acoustics,
University of Music and Performing Arts, Graz, Austria
{wendt, frank, zotter, hoeldrich}@iem.at

ABSTRACT

What influence does the directivity of a sound source have on the perceived distance impression in a room? We propose different directivity pattern designs able to modify the auditory source distance. The idea is accompanied with a comprehensive experimental study investigating the audio effect and its behavior by auralization of directional sound source and room using a 24-channel loudspeaker ring inside an anechoic chamber. In addition to the proposed directivity designs, the study covers influence of auralized room, source-to-receiver distance, signal, and single-channel reverberation. Moreover, simple room acoustical measures perform well in predicting the new effect.

1. INTRODUCTION

Our ability to localize sound sources with regard to distance is generally much less accurate than it is with direction. Literature suggests that humans underestimate distant sources while overestimating sources closer than 1 m [1]. Nevertheless, auditory source distance is a decisive feature when shaping auditory scenes with audio effects, reverberation, or new variable-directivity sound sources such as the icosahedral loudspeaker [2].

In audio technology and electro-acoustic music, the distance impression is often controlled by the amplitude and the direct-to-reverberant energy ratio (D/R-ratio). While listener are exquisitely sensitive to small amplitude changes in fine distance discrimination, recent studies suggest that the D/R-ratio provides coarse but absolute distance information [3].

As well as modifying the D/R-ratio, in extension of what has been presented by Laitinen [4], our contribution proposes directivity pattern designs able to control the room response in a greater variety. In doing so, the proposed designs are considered as an audio effect altering the auditory source distance.

This paper is arranged as follows: It briefly introduces directivities to affect the perceived auditory distance in section 2, subsequently outlines an exhaustive listening test design based on an auralized rooms and directivities in section 3, presents detailed results in section 4, and discusses influence of room and signal in sections 5, 6. Section 7 discusses the influence of additional single-channel reverberation, and the last section presents models of the experimental results.

2. DIRECTIVITY-CONTROLLED AUDITORY DISTANCE

An elegant solution to control auditory source distance has been proposed by Laitinen [4] and employs a variable-directivity source. Such a source generally influences the spatial structure of energy arriving at the listening position. In particular, this also affects the D/R-ratio, as a temporal structure.

We obtain a great variety of control by employing a directional source of various higher-order Ambisonics directivity patterns. Frequency-independent beampatterns up to the 3rd order are obtained by a combination of Legendre polynomials $P_n(\cos \vartheta)$

$$g_i(\vartheta) = \frac{\sum_{n=0}^i (2n+1) P_n(\cos \frac{137.9^\circ}{i+1.51}) P_n(\cos \vartheta)}{\sqrt{\sum_{n=0}^i (2n+1) [P_n(\cos \frac{137.9^\circ}{i+1.51})]^2}} \quad (1)$$

using the so-called max- r_E weights, cf. [5, 6], which yield a relatively narrow main lobe and sufficiently suppressed side lobes for any beam order i .

Fig. 1 shows the proposed beampattern designs that modify

- A the beam order i from three to zero for $g_i(\vartheta)$ and $g_i(\pi - \vartheta)$,
- B the ratio a/b of two opposing beams: $a g_3(\vartheta) + b g_3(\pi - \vartheta)$,
- C the angle α of a beam pair: $g_3(\vartheta - \alpha/2) + g_3(\vartheta + \alpha/2)$.

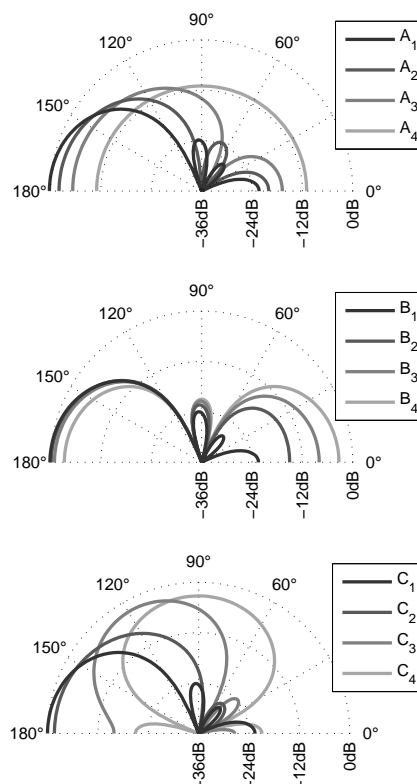


Figure 1: Directivity designs A, B, C controlling the D/R-ratio.

Table 1: Properties of tested directivity designs A, B, and C.

A	$A_{1/7}$	3 rd -order max r_E beam to/off listener
	$A_{2/6}$	2 nd -order max r_E beam to/off listener
	$A_{3/5}$	1 st -order max r_E beam to/off listener
	A_4	omnidirectional beampattern
B	$B_{1...7}$	3 rd -order max r_E beams to and off listener linearly blended at $[\infty, 6, 3, 0, -3, -6, -\infty]$ dB
C	$C_{1...7}$	two 3 rd -order max r_E beams horizontally arranged at $\pm 30^\circ \cdot [0, 1, \dots, 6]$ wrt. the listener

Table 1 lists all tested directivity designs in particular, which differently modify the amount of diffuse, lateral, and direct energy, thus the D/R-ratio. Each directivity indicated by the index 1 and 7 corresponds to a 3rd-order beam facing towards and away from the listening position ($A_1 = B_1 = C_1, A_7 = B_7 = C_7$). Furthermore, directivity pairs indicated by indices 1/7, 2/6, and 3/5 of each design are identical in their shape but horizontally rotated by 180°. Figure 1 shows the directivity patterns $A_{1...4}, B_{1...4},$ and $C_{1...4}$ normalized to constant energy.

3. EXPERIMENTAL SETUP

The effect is evaluated in a listening experiment, in which the variable-directivity source in a room is auralized using the image source method. The room is shoebox shaped with a frequency-independent absorption coefficient $\bar{\alpha}$. Specular reflections up to 3rd order are considered [7] and diffuse reflections are simulated as spherical harmonics using the software tool MCRoomSim [8]. For simplicity, diffuse reverberation of an omni-directional excitation is considered.

Playback employed a ring of 24 equally-distributed Genelec 8020 loudspeakers with a radius of $r = 1.5$ m placed in an anechoic laboratory. Each listener was sitting in the center of the arrangement with ear height adjusted to the loudspeaker ring (see Figure 3).

On the circular setup, specular reflections are auralized by the loudspeaker with nearest azimuth angle. This avoids timbral ef-

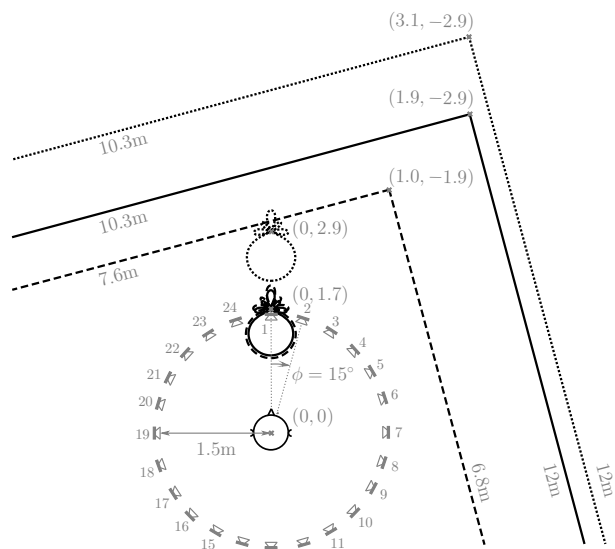


Figure 2: Room and source constellation for R_1 (—), R_2 (⋯) and R_3 (---) together with loudspeaker ring used for auralization.

Table 2: Properties of tested rooms R and signals S.

room	R_1	IEM CUBE, $T_{60} = 700$ ms, $d_1 = 1.7$ m
	R_2	IEM CUBE, $T_{60} = 700$ ms, $d_2 = 2.9$ m
	R_3	IEM Lecture Room, $T_{60} = 570$ ms, $d_3 = 1.7$ m
signal	S_1	female speech, taken from CD B&O 101, 1992
	S_2	sequence of irregular artificial bursts
	S_3	speech-spectrum noise w/ increased kurtosis

fects of amplitude panning [9]. Elevated specular reflections are attenuated in the auralization by the cosine of their elevation. The impulse response $h_l(t)$ of the l^{th} loudspeaker is obtained after superimposing specular and diffuse reflections using MATLAB. Obviously, a two-dimensional representation of a three-dimensional sound field is not optimal, but findings in [10] indicate that reflections from floor and ceiling do not have a significant influence on the auditory source distance.

Each impulse response was convolved with the sounds $S_{1...3}$, yielding a 24-channel audio file for each condition. Audio playback was controlled by the open source software Pure Data on a standard PC with RME MADI audio interface and DirectOut D/A converters.

To monitor the influence of room acoustics, three different layouts were tested, including two rooms and two source-listener distances, see $R_{1...3}$ in Tab. 2.

Geometry and reverberation time of the auralized rooms are based on the IEM CUBE, a 10.3 m \times 12 m \times 4.8 m large room with $T_{60} = 700$ ms and the IEM Lecture Room, 7.6 m \times 6.8 m \times 3 m with $T_{60} = 570$ ms.

The simulated sound source was placed near the corners of the room at a distance of 2 m and 3 m (IEM CUBE) and 1 m and 2 m (IEM Lecture Room). The listening position was chosen at a virtual distance of $d = 1.7$ m to the sound source, which already lies outside of the loudspeaker ring. Additionally, for the IEM CUBE an increased source-listener distance of $d = 2.9$ m was tested.

The listener was facing the sound source and the constellation, simulated at height of 1.8 m above the floor, had an angular offset of $\Delta\phi = 15^\circ$ with regard to the sidewalls. Figure 2 shows the setup of the auralized room using the 24-channel loudspeaker ring and Table 2 lists rooms and source-listener distances tested.

The sounds fed into auralization were female speech (S_1), a sequence of irregular bursts (S_2), and Gaussian white noise shaped to speech spectrum (S_3) as listed in Table 2. For S_3 , envelope fluctuations were slightly accentuated by multiplying the noise with its Hilbert envelope and by restriction to its original bandwidth, cf. [11]. By this procedure, S_1 and S_3 have similar spectra and kur-

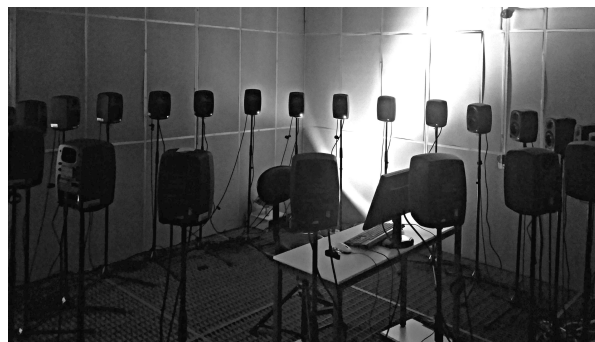


Figure 3: Experimental setup in the anechoic laboratory.

Table 3: Composition of tested sets, consisting of 7 and 9 samples.

set no.	design	index	sound	room	reverb. level
1	A	1...7	S_1	R_1	0
2	A	1...7	S_2	R_1	0
3	A	1...7	S_3	R_1	0
4	B	1...7	S_1	R_1	0
5	B	1...7	S_2	R_1	0
6	B	1...7	S_3	R_1	0
7	C	1...7	S_1	R_1	0
8	C	1...7	S_2	R_1	0
9	C	1...7	S_3	R_1	0
10	A	1...7	S_1	R_2	0
11	A	1...7	S_1	R_3	0
12	A	1...7	S_1	R_1	1
13	A	1, 4, 7	$S_{1...3}$	R_1	0
14	A	1, 4, 7	S_1	$R_{1...3}$	0
15	A	1, 4, 7	S_1	R_1	0, 1, 2

tosis, which measures the envelope fluctuation, whereas S_2 is more transient with more energy at higher frequency ($f > 1kHz$). All sounds were normalized to their RMS value for level equalization.

The above sounds are anechoic. To monitor potential influence of additional reverberation for some conditions, sound samples were reverberated before auralization. Two levels of reverberation were tested, of which level 1 corresponds to a room impulse response with a reverberation time of $T_{60} = 0.5$ s, level 2 to one of $T_{60} = 1$ s, and level 0 to the anechoic signal.

The listening test was carried out as a multi-stimulus test where listeners had to comparatively rate multiple samples, denoted as sets. Tested sets comprise 7 samples, each representing a directivity pattern, room, sound, and reverberation level (set 1 to 12, see Table 3).

To keep the testing time decent the influence of room, signal, and reverberation level was examined with the directivity design A only. In order to allow comparability and due to the absence of common reference, the data need to be normalized. Therefore additional sets comparing multiple rooms, signals and reverberation levels with directivity patterns $A_{1,4,7}$ were included. Each of these sets consists of 9 samples and is listed in Table 3 (set 13 to 15).

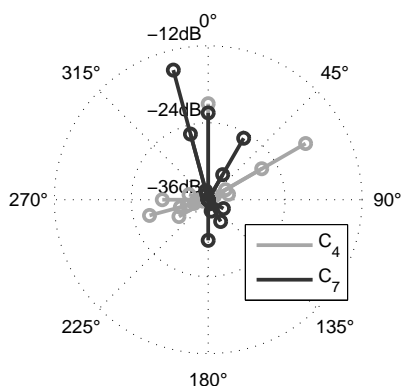


Figure 4: Direct sound and specular reflections arriving at the listening position for C_4 and C_7 , normalized wrt. C_1 .

The subjects’ task was to indicate the perceived distance on a graphical user interface displaying a continuous slider for each sample of a set to permit comparative rating along the ordinal scale *very close* (vc), *close* (c), *moderate* (m), *distant* (d), and *very distant* (vd). The subjects were allowed to repeat each sample at will, and the sound files were played back in loop.

During the listening session, the subject was requested to face loudspeaker 1 ($\phi = 0^\circ$), which corresponds to the direction of the auralized sound source.

At the beginning of the experiment, each subject was given a short training to familiarize with the evaluation scale. The training set included expected extreme values with regard to the perceived distance. Subjects were asked to rate along the whole scale and use extremes as an internal reference for further evaluations.

After the training phase, multi-stimulus tasks were presented. Each time a multi-stimulus set was displayed, the arrangement of its stimuli was an individual random permutation. The user could have the stimuli sorted by own ratings to facilitate comparative rating. The first part of the experiment consisted of the sets with 7 stimuli (set no. 1 to 12) in an individual random permutation, and the second part of the sets consisting of 9 samples (set no. 13 to 15) in an individual random permutation.

Fifteen subjects participated in the test. All of them were experienced listeners with normal hearing.

4. INFLUENCE OF DIRECTIVITY DESIGN

Fig. 5 shows a detailed analysis of the auditory source distance for the directivity designs $A_{1...7}$, $B_{1...7}$, and $C_{1...7}$ according to Table 1 and Fig. 1, based on the responses to the sets 1...3, 4...6, and 7...9 of Table 3, using all signals $S_{1...3}$ and the room R_1 . The direct comparability of all curves in Fig. 5 is feasible as all designs were determined to include reference patterns corresponding to a 3rd-order beam facing to ($A_1 = B_1 = C_1$) and off ($A_7 = B_7 = C_7$) the listening position, respectively. This allowed to linearly re-map the responses gathered in the sets 1...9 to fill out the entire interval [0; 1] for each subject. Fig. 5 shows the medians and corresponding 95% confidence intervals.

Both designs A and B yield monotonic curves. A pairwise analysis of variance (ANOVA) of the data pooled over all sounds reveals the directivity to be significant factor ($p \ll 0.01$) for $A_{1...5}$.

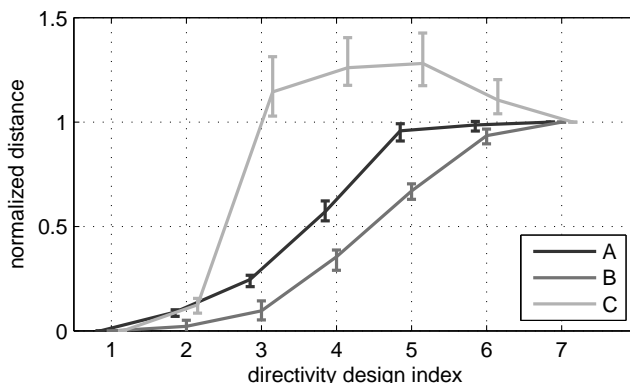


Figure 5: Median and corresponding 95% confidence intervals for all directivity designs A, B, and C, pooled over all sounds and normalized individually on directivities indicated by 1 and 7.

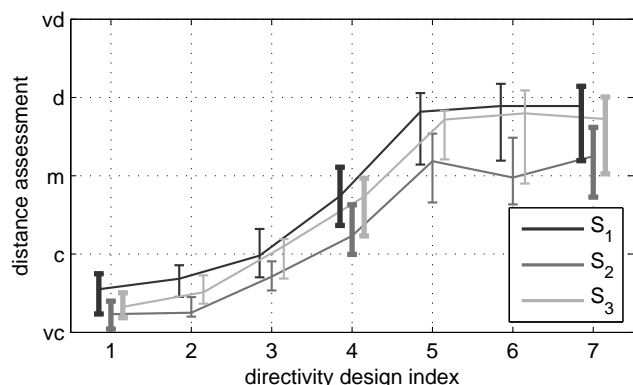


Figure 6: Median and 95% confidence intervals for tested sounds $S_{1\dots3}$ in R_1 with directivity design A .

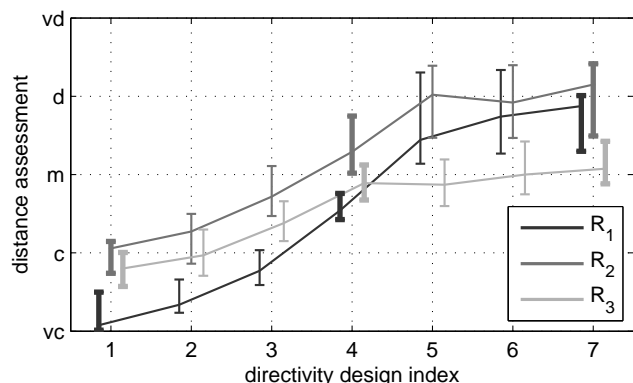


Figure 7: Median and corresponding 95% confidence intervals for tested rooms $R_{1\dots3}$ with directivity design A and signal S_1 .

For the design B , all directivities are significant ($B_{1\dots7}$, $p < 0.08$). By contrast, the curve obtained for $C_{1\dots7}$ is not monotonic in the proposed sequence. If we compare strength and angle of direct sound and specular reflections arriving at the listener for directivities C_4 and C_7 , cf. Fig. 4, we see more energy coming from lateral directions for C_4 . The more diffuse sound field explains the significant difference ($p \leq 0.04$) for $C_{2\dots6}$ compared to C_7 .

5. INFLUENCE OF THE SIGNAL

The influence of the signal $S_{1\dots3}$ on the auditory source distance of the design A in R_1 is evaluated by the stimulus set 13 in Tab. 3. As the directivity indices 1, 4, 7 of set 13 appear in the more detailed stimulus sets 1 to 3, a more detailed statistical analysis can be given in Fig. 6. Responses for indices 1, 4 and 7 (set 13) are supplemented by the linearly re-mapped responses for 2, 3, 5, 6 (set 1 to 3) for each subject, to fill out the ranges between the median values for the indices 1, 4 or 4, 7, respectively.

Fig. 6 shows the median values and corresponding 95% confidence intervals of the auditory source distance for the room R_1 and directivity designs $A_{1\dots7}$. Along the indices, the distance impression exhibits a monotonic increase for all sounds until condition A_5 . The ANOVA of neighboring values reveals conditions A_2 to A_5 as a significant factor ($p < 0.03$). By contrast, conditions $A_{5\dots7}$ do not yield a significant change ($p \geq 0.45$), despite continuously reducing the D/R-ratio. This seems to comply with a general tendency to auditorily underestimate the physical distance [1].

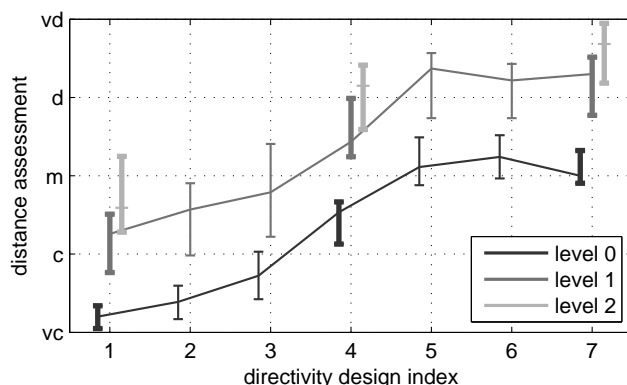


Figure 8: Median and corresponding 95% confidence intervals for reverberation levels 0, 1, 2 in R_1 with S_1 and directivity design A .

A sound-wise comparison of the obtained data reveals the significantly smaller auditory source distance for S_2 than for S_1 or S_3 ($p_{S_2/S_1} \ll 0.01$, $p_{S_2/S_3} = 0.02$). This seems to comply with the finding in [12, 13] that the auditory source distance of broadband signals decreases with the relative amount of high-frequency energy.

6. INFLUENCE OF THE ROOM

The influence of the room and the source-to-listener distance ($R_{1\dots3}$) is evaluated by the data of the set 14. Figure 7 shows the median values and corresponding 95% confidence intervals, regarding signal S_1 and directivity design A , supplemented by the linearly and individually re-mapped responses of the sets 1, 10, and 11.

A smaller room with shorter T_{60} and sound source closer to adjacent walls but with the same source-to-listener distance (R_3) leads to a flatter curve. Similar flattening accompanied by an additional offset to bigger auditory source distances is achieved by extending the source-to-listener distance (R_2). Interestingly, for all tested rooms R the directivity is a significant factor ($p_{R_1} < 0.09$, $p_{R_2} < 0.03$, $p_{R_3} < 0.04$) in the range of $A_{1\dots5}$. This significance is similar to the values obtained with pooled sounds $S_{1\dots3}$ ($p \ll 0.01$, see Fig. 6).

7. INFLUENCE OF SINGLE-CHANNEL REVERBERATION

In electro-acoustics reverberation effects are used to control depth of sounds. To get an idea how this affects the perceived distance, artificial reverberation is added to signal S_1 and tested with directivity patterns $A_{1,4,7}$ in room R_1 . Fig. 8 shows respective median values together with corresponding 95% confidence intervals. According to the ANOVA, the influence of reverberation on the auditory source distance is significant ($p < 0.05$).

Individually and linearly re-mapped responses from the sets 1 and 12 were used supplementing the responses from set 15 to provide a more detailed analysis for the reverberation levels 0, 1 in terms progression over the 7 design indices. Both reverberation levels yield a similar progression with the known saturation for $A_{>5}$. Directivity is a significant factor ($p < 0.09$) for the dry signal (rev. level 0) in the range of $A_{1\dots5}$, and by the addition of reverberation (rev. level 1), differences between the neighboring conditions $A_{1,2}$ and $A_{2,3}$ are no longer significant ($p \geq 0.16$).

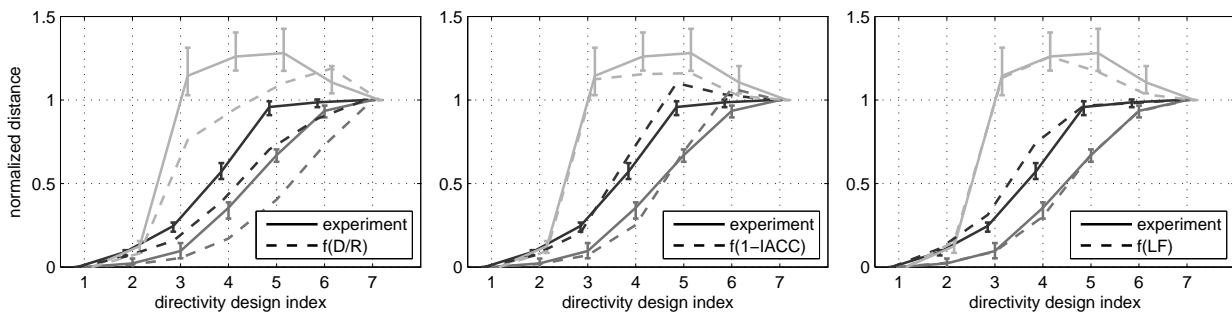


Figure 9: Comparison of Median and 95% confidence intervals for all conditions with predictors: D/R , LF , and $1 - IACC$.

8. MODELING THE AUDITORY SOURCE DISTANCE

This section discusses linear auditory source distance models for the presented effect, based on characteristic metrics of the spatial sound field and their regression to the experimental data.

8.1. Direct-to-reverberant energy ratio

The most obvious predictor in this context is the D/R -ratio. It is widely accepted for prediction of auditory source distance [1] and is defined as

$$D/R = 10 \log_{10} \frac{\int_{0ms}^T s^2(t) dt}{\int_T^{\infty} s^2(t) dt}. \quad (2)$$

By using $s(t) = \sum_l h_l(t)$, the D/R -ratio can be calculated based on the loudspeaker impulse responses, with a time constant T regarding only direct sound.

Regression analysis fits a linear regression function $f(D/R) = kD/R + d$ depending on the D/R -ratio to the normalized experimental data and yields $k = -0.049$ and $d = 0.11$. Figure 9 shows the pooled data compared with $f(D/R)$. Although the D/R -ratio and the median values of the pooled data are highly correlated ($R^2 = 0.93$) their progression along the directivity indices is qualitatively different.

8.2. Inter-aural cross correlation coefficient

As reverberation caused by the room simulation introduces binaural cues by altering the sound attributes at the two ears differentially, the inter-aural cross correlation coefficient (IACC) is used as an additional measure for auditory source distance. The IACC is based on the inter-aural cross correlation function (IACF):

$$IACF(\tau) = \frac{\int_{0ms}^{80ms} s_{left}(t) s_{right}(t + \tau) dt}{\sqrt{[\int_{0ms}^{80ms} s_{left}^2(t) dt][\int_{0ms}^{80ms} s_{right}^2(t) dt]}}, \quad (3)$$

with $s_{left}(t) = h_{left}(t) * s(t)$ and $s_{right}(t) = h_{right}(t) * s(t)$. The binaural impulse response $h(t)$ corresponds to responses for left and right ear at $\phi = 0^\circ$.

The IACC is defined as the maximum absolute value within $\tau = \pm 1$ ms:

$$IACC = \max_{\forall \tau \in [-1ms; 1ms]} |IACF(\tau)|. \quad (4)$$

Simply stated, IACC is a powerful binaural cue of the similarity between ear signals [14].

It is widely accepted that a lower IACC value leads to a bigger spatial impression, and therefore $1 - IACC$ is positively correlated with the magnitude of perceived spatial impression.

With the IACC binaurally measured in the experimental setup, linear regression yields $f(1 - IACC) = 2.23(1 - IACC) - 0.87$ to model the experimental data ($R^2 = 0.98$, cf. Fig. 9).

8.3. Lateral energy fraction

The lateral energy fraction (LF) is another acoustic measure quantifying the spatial impression. More specifically, it has been accepted as a measure of the effect of source broadening [15, 16]. Simply stated, LF is the ratio of the sum of the early lateral energy to the sum of the early total energy:

$$LF = \frac{\int_{5ms}^{80ms} s_{lat}^2(t) dt}{\int_{0ms}^{80ms} s^2(t) dt}, \quad (5)$$

with $s_{lat}(t) = \sum_l h_l(t) \sin(\phi_l)$ and ϕ_l as azimuthal angle of the l^{th} loudspeaker.

Linear regression yields $f(LF) = 7.3LF - 0.54$, cf. Fig. 9. This LF-based linear model delivers the best matching results. This is underlined by its sublime correlation of $R^2 = 0.99$.

9. CONCLUSIONS

In this contribution, an investigation was carried out into the influence of various directivity patterns on the perceived auditory distance. Two-dimensional simulation of a variable-directivity sound source was shown to provide control of the perceived auditory distance from a single point in the room. Different beam pattern designs were proposed that cause pronounced and graduated distance impressions. Additionally, the influence of auralized room, source-to-receiver distance, signal, and single-channel reverberation was studied.

The mapping of the directivity designs $A_{1...7}$ and $B_{1...7}$ to perceived distance curves is sigmoid-shaped. It resembles the compressive power functions described in [3] characterizing the relation between physical and perceived distance. Moreover, agreeing with [12, 13], signals with an increased relative amount of high-frequency energy appeared to be closer in the study.

Both decreasing the auralized room and increasing the source-to-receiver distance yield a more compressed curve, which is slight offset in case of the increased source-to-receiver distance. Despite this, the range of discriminability is persistent.

The use of single-channel reverberation is also effective at increasing the perceived auditory distance, however, it narrows the directivity-controllable range of distinguishable distance impressions.

Finally, successful modeling of the experimental results was presented. All models are highly correlated with the experimental data. Interestingly, spatial measures used to quantify the apparent source width provide very accurate predictions.

In a room, the physical distance to a source typically increases the amount of reflected sound in relation to the direct sound. Consequently, this affects the measures 1 – IACC and LF for the apparent source width, as the measurements in [17] showed. Our listening experiments only asked for distance ratings. Further research is required to determine to what extent the auditory distance and width are separable.

10. ACKNOWLEDGMENTS

The authors thank all subjects for their participation in the listening experiment. This work was funded by the Austrian Science Fund (FWF) project nr. AR 328-G21, Orchestrating Space by Icosahedral Loudspeaker.

11. REFERENCES

- [1] P. Zahorik, D. S. Brungart, and A. W. Bronkhorst, “Auditory distance perception in humans: A summary of past and present research,” *Acta Acustica united with Acustica*, vol. 91, no. 3, pp. 409–420, 2005.
- [2] G. K. Sharma, F. Zotter, and M. Frank, “Orchestrating wall reflections in space by icosahedral loudspeaker: findings from first artistic research exploration,” in *Proc. ICMC/SMC, Athens*, pp. 830–835, 2014.
- [3] P. Zahorik, “Assessing auditory distance perception using virtual acoustics,” *The Journal of the Acoustical Society of America*, vol. 111, no. 4, pp. 1832–1846, 2002.
- [4] M.-V. Laitinen, A. Politis, I. Huhtakallio, and V. Pulkki, “Controlling the perceived distance of an auditory object by manipulation of loudspeaker directivity,” *The Journal of the Acoustical Society of America*, vol. 137, no. 6, pp. EL462–EL468, 2015.
- [5] J. Daniel, *Représentation de champs acoustiques, application à la transmission et à la reproduction de scènes sonores complexes dans un contexte multimédia*. PhD thesis, Université Paris 6, 2001.
- [6] F. Zotter and M. Frank, “All-round ambisonic panning and decoding,” *AES: Journal of the Audio Engineering Society*, vol. 60, no. 10, pp. 807–820, 2012.
- [7] J. B. Allen and D. A. Berkley, “Image Method for Efficiently Simulating Small-room Acoustics,” 1979.
- [8] A. Wabnitz, N. Epain, C. T. Jin, and A. Van Schaik, “Room acoustics simulation for multichannel microphone arrays,” *International Symposium on Room Acoustics*, no. August, pp. CDROM: 1–6, 2010.
- [9] S. Tervo, J. Pätynen, A. Kuusinen, and T. Lokki, “Spatial decomposition method for room impulse responses,” *Journal of the Audio Engineering Society*, vol. 61, no. 1/2, pp. 17–28, 2013.
- [10] R. Guski, “Auditory localization: effects of reflecting surfaces,” *Perception*, vol. 19, no. 6, pp. 819–830, 1990.
- [11] A. Kohlrausch, R. Kortekaas, M. van der Heijden, S. van de Par, A. J. Oxenham, and D. Püschel, “Detection of Tones in Low-noise Noise: Further Evidence for the Role of Envelope Fluctuations,” *Acta Acustica united with Acustica*, vol. 83, pp. 659–669, 1997.
- [12] P. Coleman, “Dual Role of Frequency Spectrum in Determination of Auditory Distance,” *Journal of the Acoustical Society of America*, vol. 44, no. 2, pp. 631–632, 1968.
- [13] A. D. Little, D. H. Mershon, and P. H. Cox, “Spectral content as a cue to perceived auditory distance,” *Perception*, vol. 21, no. 3, pp. 405–416, 1992.
- [14] J. Blauert, *Spatial hearing - the psychophysics of human sound source localization*. The MIT Press, 1983.
- [15] A. H. Marshall, “A note on the importance of room cross-section in concert halls,” *Journal of Sound and Vibration*, vol. 5(1), pp. 100–112, 1967.
- [16] M. Barron and A. H. Marshall, “Spatial impression due to early lateral reflections in concert halls: The derivation of a physical measure,” *Journal of Sound and Vibration*, vol. 77, no. 2, pp. 211–232, 1981.
- [17] H. Lee, “Apparent Source Width and Listener Envelopment in Relation to Source-Listener Distance,” *Audio Engineering Society Conference*, pp. 1–6, 2013.